AD_____

Award Number: DAMD17-99-1-9007

TITLE: Combining Clinical, Sonographic, and Elastographic Features to Improve the Detection of Prostate Cancer

PRINCIPAL INVESTIGATOR: Brian S. Garra, M.D.

CONTRACTING ORGANIZATION: The University of Vermont
and State Agricultural College
Burlington, Vermont 05401

REPORT DATE: December 2002

TYPE OF REPORT: Final

PREPARED FOR: U.S. Army Medical Research and Materiel Command
Fort Detrick, Maryland 21702-5012

REPORT DOCUMENTATION PAGE

Form Approved
OMB No. 074-0188

1. AGENCY USE ONLY (Leave blank)	2. REPORT DATE	3. REPORT TYPE AND DATES COVERED
	December 2002	Final (16 Nov 98 - 15 Nov 02)

4. TITLE AND SUBTITLE
Combining Clinical, Sonographic, and Elastographic Features to Improve the Detection of Prostate Cancer

5. FUNDING NUMBERS
DAMD17-99-1-9007

6. AUTHOR(S)
Brian S. Garra, M.D.

7. PERFORMING ORGANIZATION NAME(S) AND ADDRESS(ES)
The University of Vermont and State Agricultural College
Burlington, Vermont 05401

E-Mail: bgarra@zoo.uvm.edu

8. PERFORMING ORGANIZATION REPORT NUMBER

9. SPONSORING / MONITORING AGENCY NAME(S) AND ADDRESS(ES)
U.S. Army Medical Research and Materiel Command
Fort Detrick, Maryland 21702-5012

10. SPONSORING / MONITORING AGENCY REPORT NUMBER

11. SUPPLEMENTARY NOTES
Original contains color plates: All DTIC reproductions will be in black and white.

12a. DISTRIBUTION / AVAILABILITY STATEMENT
Approved for Public Release; Distribution Unlimited.

12b. DISTRIBUTION CODE

13. ABSTRACT *(Maximum 200 Words)*

The goal of this project is to combine features derived from ultrasound (US) images, US radio frequency (RF) data, tissue elasticity imaging, and clinical data such as PSA into a computerized system for displaying prostate images that indicate probable location(s) of cancer. RF data are acquired from in-vitro prostatectomy specimens in cross sectional planes 2mm apart. These data are used to calculate RF features such as backscatter coefficient and are also used to generate images and elastograms from which image texture features and tissue strain are computed. These features are correlated with histology from the same location in the prostate to determine which feature combinations accurately predict the presence of cancer.

Numerous personnel and subcontractor problems were encountered from the beginning of the project. These combined to delay the project while the PI and newly recruited investigators developed the expertise needed. Despite these delays, 3D US RF data were acquired in over 100 prostates along with accurately registered 3D pathology data and correlative clinical data. Software for accurately registering pathology and US in vitro was developed and preliminary results show that RF features can be used to distinguish cancer from benign prostatic tissue. In the past year, a new method for reducing the variance in elastographic strain was developed allowing the incorporation of strain as a key additional feature for cancer detection. Also, a new collaboration between UVM and Inserm (France) has provided software to calculate elastograms from a curved compressor. This will finally allow the testing of features from curved array endorectal probe data.

14. SUBJECT TERMS
Prostate cancer, ultrasound, elastography, tissue characterization

15. NUMBER OF PAGES
38

16. PRICE CODE

17. SECURITY CLASSIFICATION OF REPORT	18. SECURITY CLASSIFICATION OF THIS PAGE	19. SECURITY CLASSIFICATION OF ABSTRACT	20. LIMITATION OF ABSTRACT
Unclassified	Unclassified	Unclassified	Unlimited

FOREWORD

Opinions, interpretations, conclusions and recommendations are those of the author and are not necessarily endorsed by the U.S. Army.

___ Where copyrighted material is quoted, permission has been obtained to use such material.

___ Where material from documents designated for limited distribution is quoted, permission has been obtained to use the material.

___ Citations of commercial organizations and trade names in this report do not constitute an official Department of Army endorsement or approval of the products or services of these organizations.

___ In conducting research using animals, the investigator(s) adhered to the "Guide for the Care and Use of Laboratory Animals," prepared by the Committee on Care and use of Laboratory Animals of the Institute of Laboratory Resources, national Research Council (NIH Publication No. 86-23, Revised 1985).

X For the protection of human subjects, the investigator(s) adhered to policies of applicable Federal Law 45 CFR 46.

N/A In conducting research utilizing recombinant DNA technology, the investigator(s) adhered to current guidelines promulgated by the National Institutes of Health.

N/A In the conduct of research utilizing recombinant DNA, the investigator(s) adhered to the NIH Guidelines for Research Involving Recombinant DNA Molecules.

N/A In the conduct of research involving hazardous organisms, the investigator(s) adhered to the CDC-NIH Guide for Biosafety in Microbiological and Biomedical Laboratories.

(electronic signature) 13 Dec 2002

TABLE OF CONTENTS

INTRODUCTION

The ultimate goal of this project is to combine features derived from ultrasound (US) images, US radio frequency (RF) data, tissue elasticity imaging, and clinical data such as PSA into a computerized system for displaying prostate images that indicate probable location(s) of cancer. Each of these different classes of features has been shown to be useful for prostate cancer detection. By combining those features in each class that perform best in a set of test cases, we hope to develop an accurate tool for detecting regions on the ultrasound image that a high probability for cancer. Eventually we hope these techniques will be used to rapidly identify high probability areas and mark them on the ultrasound image in real time or near real time.

This project began by gathering RF data from in-vitro prostatectomy specimens in cross sectional planes 2mm apart using a linear array transducer. These data are used to calculate RF features such as power spectrum slope, and backscatter coefficient at each location in the gland. The data are also used to generate images and elastograms from which image texture features and tissue hardness features are computed. The features are correlated with histology taken at the same tissue planes to determine which features and feature combinations most accurately predict the presence of cancer. The various image, hardness, and RF features will later be combined with prior probability information derived from an AFIP 3D model of prostate occurrence and with clinical PSA values to produce a system that can accurately identify the presence of prostate cancer using ultrasound data.

After developing the techniques to perform identification of prostate cancer using the linear array scans, our plan is to migrate the technique to data obtained from a curved array endorectal transducer. The ultimate goal of all the in-vitro work is to demonstrate a system using an endorectal prostate probe that will be able to mark areas of high probability for cancer on each ultrasound image. This will prepare us for an in vivo study directed at developing an ultrasound system that can better direct biopsies of the prostate gland to areas of high likelihood for actual prostate cancer.

During the project, it we have become impressed with the importance of obtaining high quality RF data both from linear and curved array transducers in a manner that will give reliable RF, texture and elastographic features that will be usable in a machine based classification scheme. The critical need for reliable high quality data has forced us to begin acquisition of new data each time a new problem with processing surfaced that required an alteration in the data acquisition approach. This has occurred several times (including twice in the past year) as we learned more about the complexity in interdependence of features on the acquisition method. But we feel that new acquisition procedures are behind us and that we can move towards migrating the technique to curved array transducer data as soon as we complete a series of phantom experiments to verify the accuracy of our process for registration of US data and pathology. This final phase of the project will be performed in coming months along with additional work pertaining to a PhD Thesis being prepared by the graduate student, Mr. He.

RESEARCH ACTIVITIES SUMMARY

Administrative Overview:

The administration of this project has been complex with many issues and delays to deal with including the loss of key personnel, a lengthy administrative delay in starting the project, hiring problems, and the failure of subcontractors to deliver required services or components. A year-by-year summary of activities and issues follows:

Year 1 (11-98 to 11-99):
Start Delay: Although the contract was awarded in November of 1998, University Administrative problems prevented the PI from gaining paid faculty status until 1 May 1999. This prevented the PI from obtaining lab space, or hiring an assistant until that time. In May and June 1999, a lab assistant was hired, space was found, and equipment components lost in the year since moving to Vermont were replaced. Actual acquisition of in vitro prostate data was begun in July 1999--7 months later than planned.

George Washington University Contract Cancellation: After the contract was awarded in November 1998, the postdoctoral researcher, Rash Mia, informed us of his intent to leave academics for industry. George Washington University was instructed to find a replacement for Dr. Mia as most of the development work was to have been performed by him. In October 1999, a call to GWU was made to determine if a replacement had been found. Finding that a search for a replacement had not even begun and that the PI at GWU was in not even in the country, I decided to cancel the contract and begin a search for a person who could perform the work at UVM. Contacting the Department of Mechanical Engineering, a Chinese student was recommended as a possibility. Lacking other candidates and with time passing quickly, I concluded an agreement with Mechanical Engineering to bring the student from mainland China to participate in the project beginning in January 2000.

Year 2 (11-99 to 11-2000)
Training Delays: Due to Visa issues, the graduate student, Mr. Zhi He, did not arrive in the US until April 2000. Once he had arrived, it was clear that his language and mathematics skills were not at the level we expected and additional training would be required. Also, the new graduate student had many required courses to take as part of his graduate training. Training in ultrasound, image processing and the MATLAB programming environment continued throughout the summer, culminating in a trip to Rockville, MD to continue training in collaboration with other investigators on the team (Drs Wagner and Wear). Real work on the signal processing and data fusion portions of the project (tasks 2, 4, and 5) began in October 2000, nearly two years later than expected originally.

Pathology Delays: Although the Department of Pathology had originally agreed to handle histology preparation, interpretation, and assembly of quarter sections into whole mount equivalents for comparison with US data, it became apparent in mid 2000 that the work was not progressing. Slides were being made and interpreted by Dr. Trainer, but the image assembly work was stalled for lack of a person to perform the work. Rather than risk further delay, the pathology image assembly was

taken over by the PI and the research assistant, with training by Dr. Tuthill of the cell biology laboratory. After this decision in summer of 2000, some delay in getting started due to difficulties in changing the position description of the laboratory assistant, equipment procurement for the task and training. By December 2000, the work of assembling the pathology images was underway.

Year 3 (11-2000 to 11-2001):

Efforts in the third year of the project were focused on:

a. Continuing the clinical data acquisition begun in June 1999
b. Continuing to work with Mr. He, the graduate student to refine the software to compute the ultrasound based features
c. Completing development of a system for correlating ultrasound features with pathology on "whole mount equivalent sections" made by reassembling pathology slide sections.

We succeeded in developing this system plus the appropriate software, and preliminary results were reported in June 2001 at the Ultrasonic Tissue Characterization Symposium in Rosslyn, VA[1].

Preliminary analysis of RF backscatter was carried out using this software and Mr. He then took the summer to write his masters thesis based on the work, which was completed in September 2001 and accepted by the graduate college in October 2001. Mr. He received his master's degree in October for the work.

Development of a user-friendly interface for the software consumed a significant amount of Mr. He's time forcing him to devote less time to the critical questions of ultrasonic feature computation and software testing. To assist with these software development issues, a programmer (Mr. Steven Felker) was hired on a part time basis to assist with file conversion software, and graphical user interface software development to allow Mr. He to focus more on feature computation and data fusion issues.

Personnel changes:
The complex process of combining the quarter section pathology slide images into the equivalent of whole mount sections for comparison with the ultrasound images and data was performed by the laboratory assistant Gorana Skjlarevski. She made considerable progress but suddenly left the project in June 2001. This brought to a halt both ultrasound data acquisition and pathology image processing. A search for a replacement was instituted and in September 2001, Mr. Steven Knight was hired. The principal investigator trained Mr. Knight in the ultrasound data acquisition from prostatectomy specimens over a four-week period and Mr. Knight also received training from Dr. Tuthill on pathology image reassembly. Unfortunately, after the training period, Mr. Knight performed only two ultrasound acquisitions in two months and performed no pathology image assembly. It was clear that because of other workload and personal problems that Mr. Knight could not perform the jobs expected of him so he was asked to resign in late November and tendered his resignation shortly thereafter.

Year 4 (11-2001 to 11-2002):

A search for a replacement began and in January 2002, Ms. Sarah Grimm was hired. Training in both ultrasound data acquisition and pathology image assembly was begun immediately and continued through Jan and February 2002. Prostate acquisition was restarted in March 2002 and Pathology image assembly was restarted in April 2002.

In the meantime, Mr. He, now a Ph.D. student continued work on the user interface and verification of accuracy of RF feature computations. He also began to define his Ph.D. thesis based on the work on this project.

Consultant issues: A key feature of the project was our intent to include elastographic features in our classifier for prostate cancer. Jonathan Ophir, a pioneer in the field of elastography was hired as a consultant with the task of providing a modern version of software to compute elastograms with lateral displacement correction. The older version of software we already had could not perform lateral correction. Despite repeated requests for the software, and payment of 2/3 of his project consulting fee, Dr. Ophir never provided the required software. The PI attempted to enlist the aid of another elastography researcher, Elisa Konofagu at Harvard, in the task but Dr. Konofagu did not have sufficient time to devote to the project. While a solution to this problem was being sought, Mr. He added code to compute basic (non lateral corrected) elastograms to our existing software package. This allowed us to study the critical problem of excessive variance in elastographic strain values enabling us to find a solution to the problem of how to make heretofore subjective elastograms both quantifiable and reproducible. The first half of 2002 was spent devising experiments to test various methods of elastogram quantification. This work was reported at the 2002 International Tissue Characterization Symposium in June 2002[2]. The problem of obtaining software to compute highly corrected elastograms was solved in October 2002 with an agreement to swap our registration software for advanced elastography software. This agreement was reached with Remi Souchon, Research Unit U556, Inserm Therapeutic Ultrasound Research Laboratory (France). This group at Lyon, France, was independently pursuing prostate cancer elastography as a guide to treatment with high intensity focused ultrasound. From here on, we will be closely collaborating with the Lyon group in the development of advanced prostate elastography. Advanced elastography software will be critical for analysis of data acquired from curved array endorectal transducers.

In finding a way to quantify and improve reproducibility of the tissue strain feature obtained from elastography, we found that we once again had to significantly modify our RF acquisition scheme. This caused us to delay acquisitions with a curved array transducer until a new series of acquisitions using the new method and the linear array transducer could be completed. That series is now complete and we can move to acquiring with both linear and curved array transducers.

In summary, the first two years of the project were beset by unexpected delays and personnel losses. We have made steady progress since that time and now seem to have for the first time trained people working on each aspect of the project and a sizeable body of. We are in a position to continue working without further financial support for the next nine months and hope to complete in that time the refinement of classifiers to distinguish prostate cancer from benign tissue, several papers reporting results, initial analysis of results using RF data from curved array transrectal ultrasound transducers, and data acquisition and processing for Mr. He's Ph.D. thesis.

PROJECT RESEARCH SUMMARY

Task 1 (Months 1-6): Collect RF data on 25 prostate glands with the linear array transducer. Develop a preliminary plan for data acquisition for tasks 5 and 7.

This part of the project has been completed but had to be repeated twice, once because of data corruption caused by inadequate dynamic range in the digitizer system, and once because of changes in acquisition methodology required to obtain reproducible data for elastography.

Initially, the plan was to acquire the data with the anterior surface of the gland facing the transducer. This resulted in shadowing that interfered with visualization of the posterior part of the gland where the peripheral zone is located. Since the peripheral zone is a critical area for the development of prostate cancer, we decided to change the orientation of the gland so that the posterior surface was closest to the transducer. In doing this, other problems surfaced. One serious problem was that the first 3-4 mm of distance from the transducer yields inferior data due to reverberation artifacts and due to the wider beamwidth at that location. An ultrasound standoff was needed, but the standoff would have to be stiff enough to allow compression of the prostate gland while still being similar in density to the adjacent prostate gland so that a reverberation artifact would not appear within the prostate gland data.

This was accomplished by producing a plastic casting containing a cavity for the standoff gel (Figure 1). The casting is attached to the transducer and a block of solid gel cut from a commercial disposable gel pad (Aquaflex, Parker Laboratories) is inserted into the cavity (held in by friction) and is coupled to the transducer with standard ultrasound gel. The solid gel forms a surface stiff enough to use as a compressor during elastography RF acquisition, but without reverberation artifacts. To further minimize the effects of acoustic shadowing in the prostate gland, a 5MHz transducer rather than a 7.5MHz transducer is used. The 5 MHz transducer gives a lower resolution ultrasound image, but high quality RF data for elastography and for RF analysis.

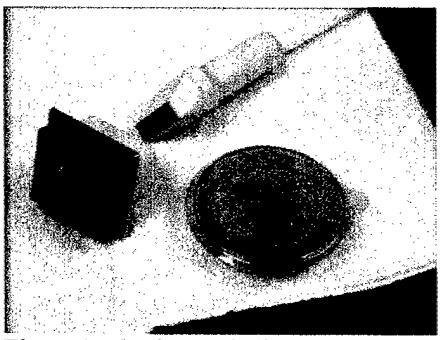

Figure 1: plastic standoff holder, transducer and gel pad

One possible serious issue was the lack of supporting tissue around the prostate gland during acquisition of the RF data for elastography. In all previous work on prostate, elastograms have been generated from data acquired from a prostate gland embedded in a gelatin block. The

gelatin block provides support for the gland to prevent sideways movement, a flat surface against which to compress, and an automatic acoustic standoff.

It is impractical to embed a clinical prostate specimen in gel however since the pathologists must examine and ink the surface of the gland prior to preparing it for histologic sectioning. In addition, the gel would have to be completely removed for proper fixation of the prostate gland later in pathology. Also, the heat of the gel embedding process might alter the microscopic appearance of cells leading to errors in diagnosis. For these reasons, our project proposed scanning the glands in sterile saline without the normal supporting gel block but a big concern was whether a useful elastogram could be obtained at all by this method.

Figure 2 below shows that quality elastography IS possible using our technique. Some artifacts occur due to the contact of the flat compressor mainly with the center of the prostate gland but we believe that this effect can be corrected for. We expect that even higher quality elastography can be achieved with the new software being provided by R. Souchon (Lyon, France) as part of the collaboration outlined in the administrative section above.

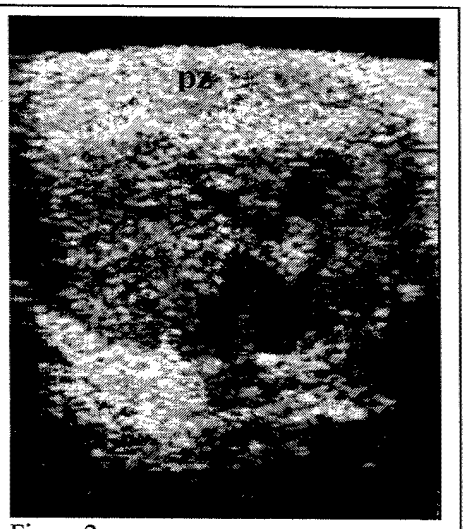

Figure 2a.

Figure 2b.

Figure 2: Large prostate gland with a prominent central zone on b-scan (a) and high-resolution elastography (b). Note that the central zone has a hardness similar to the peripheral zone (pz) and that the verumontanum/urethra (vu) appears as a bright focus on the elastogram. On the elastogram harder areas are dark and softer areas are bright.

In early 2001, the software for processing the RF data from the prostates already acquired, had reached a sufficient level of reliability to begin processing. Problems with the data already acquired immediately surfaced. Despite being trained to avoid setting the gain too high, the laboratory assistant had done so on the ultrasound machine and most of the RF waveforms were clipped, being beyond the range of the 8 bit Lecroy to digitize. This flaw rendered most of the already acquired data useless for RF analysis although the data can still be used for elastography. The problem was traced to the fact that gain was being set based on a subjective evaluation of the

image on screen, and this was affected by room lighting. Software was then developed to allow immediate viewing of the acquired RF waveforms so that waveform clipping can be detected and corrected before acquisition begins. Since the goal of the project is to use multiple features including RF features, another group of prostates had to be acquired.

The most recent change is acquisition was to improve the reproducibility of elastographic strain data computed from the RF signal. Extreme variability in strain values was noted once the software to quantitatively compute the feature was developed in early 2002. A method to reduce the variance was eventually developed, but this once again required a change in acquisition procedure. So an additional set of patients had to be acquired using the new method so that elastographic strain could be added to the feature set. This set of new patients has just been completed. Luckily, there is a way that the prior strain values can be corrected retrospectively to reduce their variance once we have the new prostate data.

Task 2 (months 1-6): Develop a methodology for registering optical pathology information with ultrasound data.

A procedure for registering optical pathology information with ultrasound data has been developed. It now consists of the following steps:

1. The prostatectomy specimen is fixed in formalin.
2. The gland is sectioned every 2-3mm after coating the surface of the gland with inks of various colors to identify anterior and posterior surfaces
3. Each 2-3mm thick whole cross section is divided into quarters.
4. The quarters are labeled and embedded in paraffin
5. The embedded quarters are sectioned and mounted onto glass slides
6. The slides are stained and examined by the pathologist—Dr. Trainer
7. Areas of cancer are marked on the slides in indelible ink
8. The slides are digitized by placing them on a flatbed scanner and scanning at 300dpi. This produces pathology images of high enough resolution without producing unnecessarily large image files—see figure 3.
9. The slide images (including identification labels indicating the original slice position and quarter) are imported into Adobe Photoshop and reassembled into complete cross sections ("whole mount equivalents").
10. The whole mount equivalent images are placed into a database on a shared disk drive for later comparison with ultrasound data.

An example of a "whole mount equivalent" image assembled from quarter sections is shown in figure 4.

Figure 3. Scanned in images of the four quarters of a pathology slice before reassembly into a complete cross section. Areas of cancer are marked in with blue ink outlines.

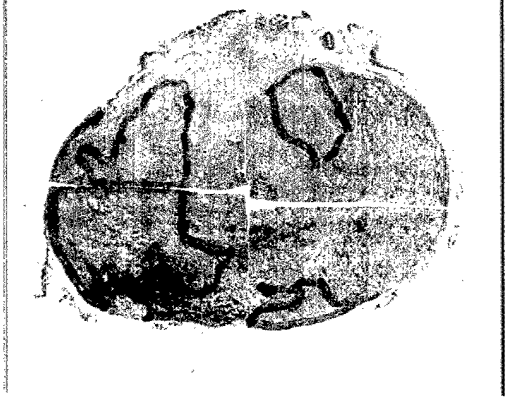

Figure 4. Quarter sections reassembled into complete cross-section (whole mount equivalent). Cancer areas marked by blue lines

A few modifications to the original procedure outlined in the prior report were made. No warping of pathology images was performed due to concerns by the pathologists that such a procedure might introduce undesirable distortions into the pathology data. Thus some of the whole mount equivalents have gaps where the quarter sections did not fit precisely with one another. This has not proved to be a problem for correlation with ultrasound data. When looking for benign or malignant areas, the gaps are simply avoided.

Once the whole mount equivalent pathology images have been created, the problem of matching them to corresponding US data remains. Initially, our plan for registering the US prostate data with pathology data called for defining the first image of the prostate by sewing silk or prolene suture into the capsule of the prostate at four locations along the plane of the first slice. These sutures would then be used to line up the plane of the first scan so that it would be

slice. These sutures would then be used to line up the plane of the first scan so that it would be perpendicular to the long axis of the gland and would also be used by the pathologists to locate the position of their first slice through the gland. In practice, the procedure proved to be too cumbersome and time consuming to allow us to promptly scan the glands. Instead, one or two sutures are sewn into the capsule near the apex of the gland. Then the gland is carefully lined up in the water tank so that the scan planes are perpendicular to the long axis of the gland. The scan containing an image of the sutures is identified (typically the second or third slice) and is used to correlate slice position with pathology. For example, slice three on the ultrasound may contain the image of the suture whereas slice 2 of the pathology may contain the suture. In this situation, ultrasound slice 2 corresponds to pathology slice three. The other slices are related to each other by taking the ratio of the number of slices taken through the gland. For example, if 15 slices are taken using ultrasound and only 12 were taken in pathology, the spacing between slices is 2mm for ultrasound and 15/12 x 2mm = 2.5mm for the pathology slices. The ultrasound slices correspond to pathology according to the table 1 below:

Table 1: Example of ultrasound/pathology data correspondence (for case of 15 US slices and 12 pathology sections where sutures are seen in US slice 3 and path slice 2)

US Slice	Position in Gland (mm)	Corresponding Path Slice(s) (position in parentheses)
1	0	none
2	2	1 (1.5)
3	4	2
4	6	3 (6.5)
5	8	4 (9)
6	10	4 (9)
7	12	5 (11.5)
8	14	6
9	16	7 (16.5)
10	18	8 (19)
11	20	8 (19)
12	22	9 (21.5)
13	24	10
14	26	11 (26.5)
15	28	12 (29)

In most cases, foci of prostatic cancer are large enough to appear on several consecutive slices making correlation of ultrasound data with pathology relatively straightforward.

Due to the US transducer beamwidth, the suture may be visible on two adjacent ultrasound slices. This introduces further uncertainty into the exact pathology slice with which the ultrasound data should be correlated. The solution to this problem is to only use cancer foci that are large enough to appear on several pathology slices. Then the ultrasound slices lying closest to the center of the lesion at pathology are used to identify ultrasound data coming from a cancer. This reduces the

possibility that ultrasound data coming from normal prostate tissue will be misclassified as cancerous during the classifier or neural network training process.

Once the matching histology and ultrasound "slices" were found, the following procedure for finding the ultrasound RF data to be classed as "cancer" is used:

1. After the histologic sections have been reassembled with ink marks on cancer areas, match each section to the corresponding "slice" of ultrasound data.
2. Adjust the histologic image to conform to the shape, size and orientation of the ultrasound image and confirm that the images match with respect to shape, rotation and size. Mark out a region on the histologic image lying within a region previous marked as cancer and find the corresponding region on the ultrasound image. Process only that RF data for texture features and RF features.
3. Evaluate the RF and texture features for features that seem to discriminate between cancer and normal tissue.

Regions selected from normal areas of the glands are used to gather data about the RF, Texture, and strain values of normal prostatic tissue.

Software to perform the selection a corresponding pathology whole mount equivalent image based on the registration scheme described in the 2000 report has been developed and successfully used. See task 4 description for further discussion.

A significant source of potential error in registration lies in the care with which the steps of the procedure outlined above are followed. Of major concern is the initial sectioning of the prostate gland in pathology after formalin fixation (step 2 in the procedure above). If this is done incorrectly -- for example if the sections are not plane parallel and are not in the same plane as the ultrasound data acquisition, significant misregistration errors could develop. There is potential for errors since several at least three different persons in pathology have been responsible for sectioning the gland.

We are currently performing experiments to test the actual accuracy of the data registration system that we use. A prostate phantom is constructed out of a slab of beef, two small nodules of rubber are inserted and the phantom is then scanned and sectioned just as would a prostate gland. The nodules are designed to be visible to the eye, on ultrasound images, to the pathologist, and on elastography. By determining the difference in nodule position on US vs. the position on the whole mount section, an estimate of registration error can be made. Some difficulty was encountered finding a "nodule" that was visible by all modalities. Our first test was unsuccessful due to technical difficulties; the next test should yield the desired positional error information.

In Summary, a method for registration of histologic information with ultrasound raw data has been developed and is in use in other phases of the project. Task 2 is complete.

To reveal the spatial pattern of localized prostate cancer distribution, a three-dimensional (3-D) statistical volumetric model, showing the probability map of prostate cancer distribution together with the anatomical structure of the prostate, has been developed from 70 digitally imaged surgical specimens. Through an enhanced virtual environment with various visualization capabilities, this master model permits for the first time an accurate characterization and understanding of prostate cancer distribution patterns. The construction of the statistical volumetric model is characterized by mapping all of the individual models onto a generic prostate site model, in which a self-organizing scheme is used to decompose a group of contours representing multifold tumors into localized tumor elements. A crucial step in creating the master model is the development of an accurate multi-object and non-rigid registration/warping scheme incorporating various variations among these individual models in true 3-D. This is achieved with a multi-object based principle-axis alignment and an affine transform, and followed by a thin-plate spline interpolation driven by the surface based deformable warping dynamics. Based on the accurately mapped tumor distribution, a standard finite normal mixture is used to model the cancer volumetric distribution statistics. The process is graphically outlined in Figure 3 below:

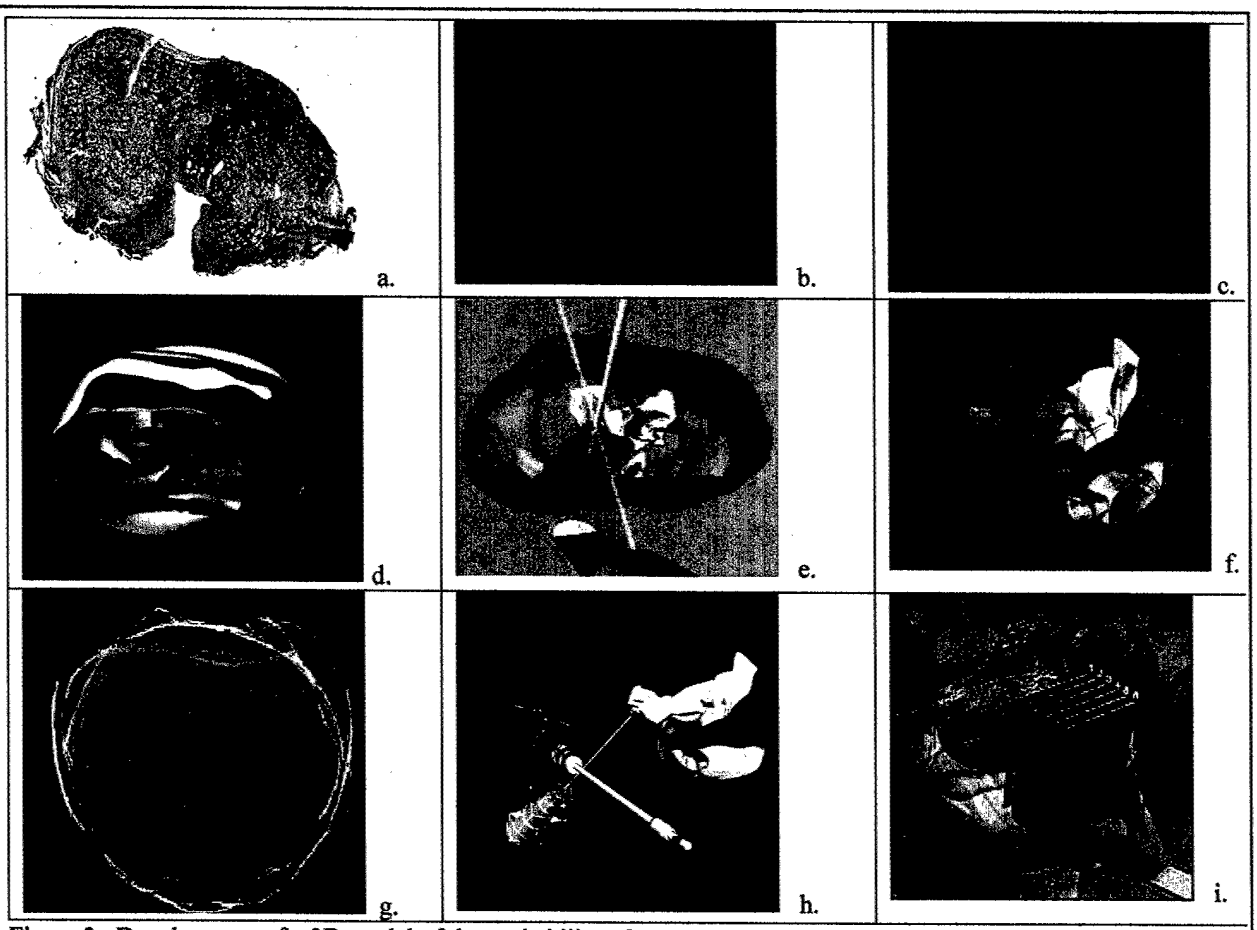

Figure 3. Development of a 3D model of the probability of prostate cancer. a. digitally imaged surgical specimens, b. decomposition of tumor contours, c. reconstruction of multifocal tumors, d. prostate site model in 3D computer graphics, e. TRUS based biopsy simulation virtual environment, f. display of multifocal tumor distribution, g. 3D statistical volumetric model of tumor spatial distribution -- data from this model will be used to calculate prior probabilities for the current study, h. biopsy planning, i. Model guided biopsy-- in our proposal actual ultrasound data with the added model data will be used.

The above has already been accomplished with the AFIP data. Still remaining is to align the model with our prostate US data set. This work has yet to be accomplished by Dr. Lo, the investigator responsible for this component. We have delayed this component to give us time to add our 3D data to the model. Also, though the probability distribution map has not yet been fused to our US data, it is not needed at this point since incorporation of prior probabilities is needed only in the final phases of UNKNOWN region of interest classification and we are still in the phase of computing features for KNOWN regions of interest to determine which features best discriminate cancer from benign tissue.

Initially, we were planning to do our own 3D modeling of the prostate cancer probability data that we are acquiring as part of this project. That will be delayed to a future project since we have no one available to work on that sizeable task.

Task 4 (months 1-9): Software development. Adapt existing RF analysis software and incorporate texture analysis. Develop software to automatically calculate RF and texture features over multiple subregions in an image.

Rather than adapt existing RF analysis software, it turned out to be more educational and expedient to develop new software based on MATLAB to compute both RF and Texture features. Taking ideas and some code from prior work done by Drs. Rash Mia and Keith Wear, Mr. He took command line driven programs and converted them to software that would run using a graphical user interface. The initial version, which was completed in October 2000, computed multiple features from a region of interest drawn on the ultrasound image. The user interface for this is shown in figure 5

Figure 5. Example of the graphical user interface to be used for prostate ultrasound data processing.

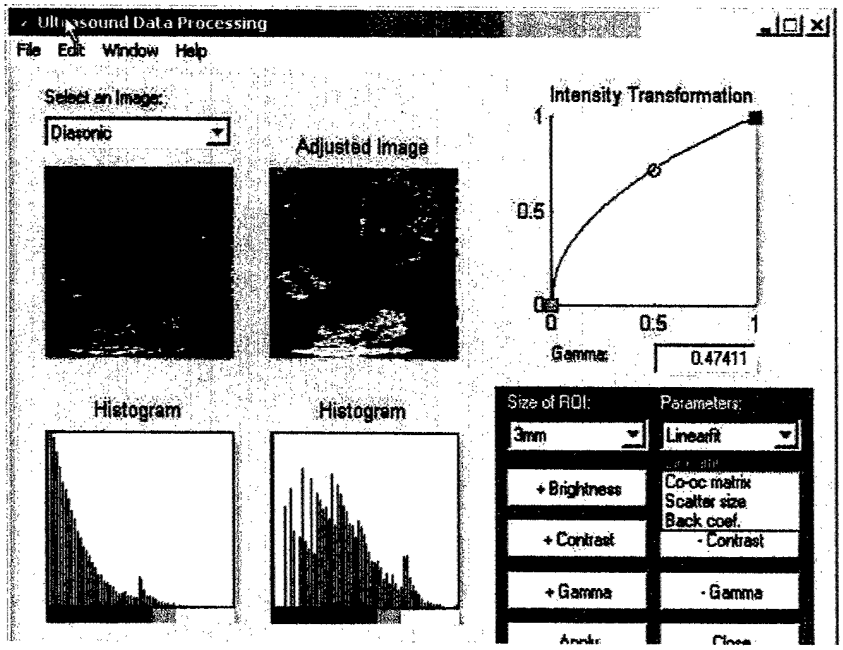

This software gave us the opportunity to test feature computation algorithms, but it did not allow a user to correlate the ROI drawn on the ultrasound image with pathology. We decided that a better approach would be to draw a region of interest on the pathology image (in which cancerous regions are already outlined) and then find the corresponding area in the ultrasound RF data. Therefore, the user interface above was completely revamped to include the pathology image and allow regions of interest to be selected from that image.

This revised software, which was designed to allow a user to identify a normal or cancerous area on the pathology image and find the corresponding region in the ultrasound RF data set, was completed in April 2001 and used successfully to analyze ultrasound data. The software was developed in MATLAB with a Windows Graphical User Interface. To calculate RF or texture features the user selected the ultrasound data file that he/she wished to use. The software automatically selected the pathology slice that most closely corresponded to the ultrasound data based on the slice correlation scheme described in task 2 above. The user then adjusts the size of the pathology image to match the ultrasound image by drawing a box around the image of the prostate that touches the image of the gland on all four sides. The pathology image is then oriented to match the ultrasound data—this usually involves rotating the pathology image 180 degrees. The user then draws are region of interest on the pathology specimen and specifies whether it is a cancerous or benign region. The software automatically finds the corresponding region on the corresponding ultrasound image, finds the raw RF data corresponding to that region, and computes RF and textures features from the RF data and places the results in a data base. It is also possible to draw multiple regions and then have the software process the RF for all regions of interest at a later time as a batch process. Figure 6 shows the new GUI interface.

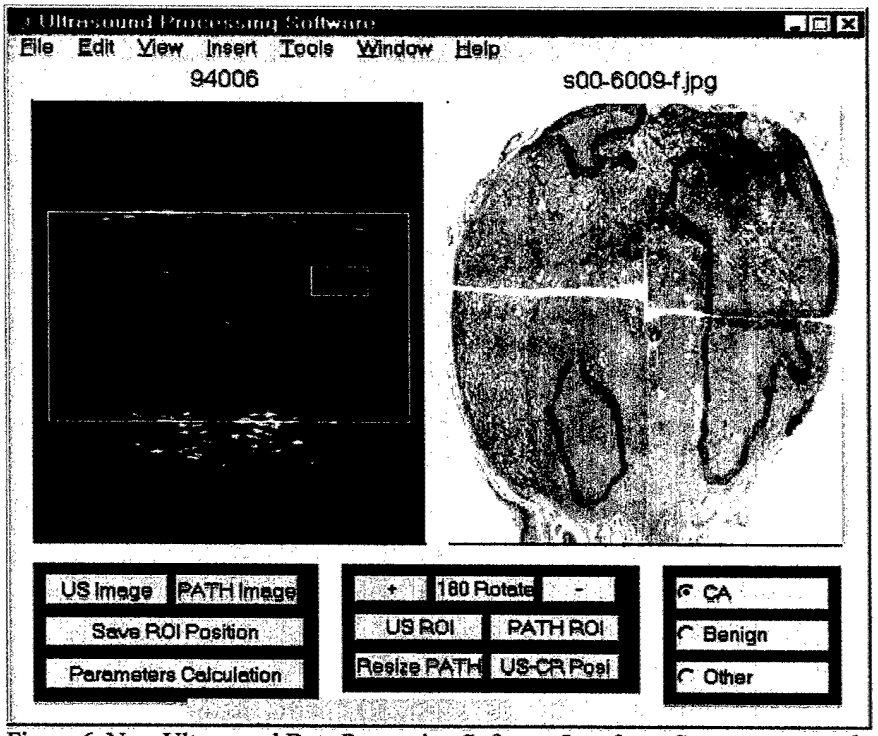

Figure 6. New Ultrasound Data Processing Software Interface. Screen capture of the interface used to process ultrasound data from defined regions. The pathology image on the right side has a square region of interest drawn (dotted box) and a region of cancer. The corresponding ultrasound data is denoted by the box drawn automatically on the ultrasound image (left).

Of course, although this new user

Of course, although this new user interface was designed to let the user process selected regions of interest so that a database of features values for cancer and benign tissue could be generated, the software is also capable of processing RF data from entire slices or multiple slices, automatically subdividing the data into subregions and calculating features for those regions.

The software outlined above was used to analyze a large subset of our acquired data to verify correct operation of the software and to begin to determine the most useful feature combinations as outlined in Task 7. See task 7 description for our preliminary results. Based on these results, one important modification was made in the way the software computes features. In previous versions, the region of interest size was variable and controlled by the size selected by the user. Evidence that ROI size biases the feature results prompted us to allow uses to select an ROI but features are computed from subregions of the ROI of FIXED size to eliminate this bias.

In summary, task 4 is essentially complete. Additional modifications to the software needed for fusion with elastographic data were made as described below. Additional refinement and testing of the algorithms for computing individual features is ongoing.

Task 5 (months 12-18): Data Fusion

Having developed the software to use pathology images to select data for RF processing in early 2001, we began the process of development of data fusion software to combine elastography results with RF results in user-selected regions of interest. Having had success, with an interactive scheme for orienting pathology images with those from ultrasound RF data, we have elected to initially use the same approach for elastography, processing the elastographic data separately using software from the University of Texas and combining those results with those from the RF analysis. In late 2001, we completed the development of software that calculates RF and texture features from data corresponding to a user selected region on a pathology image AND selects the appropriate region from the corresponding elastographic image placing the mean strain value from the elastogram ROI into the feature database (figure 7).

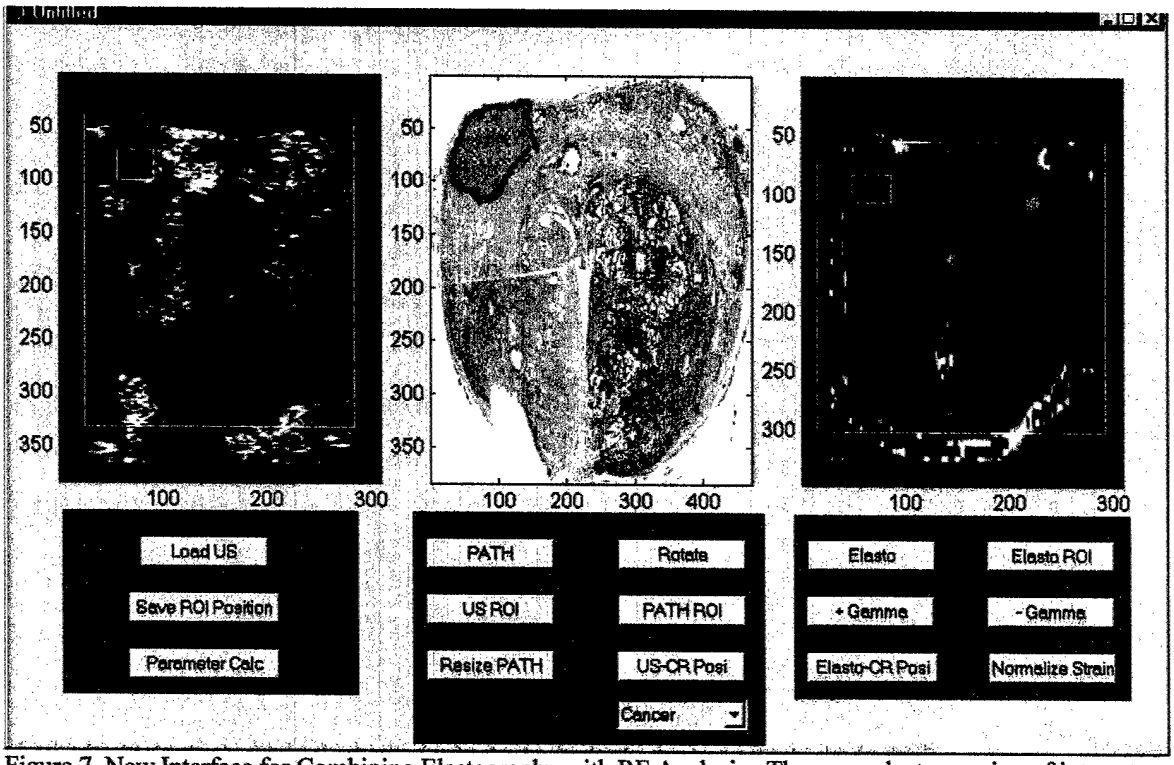

Figure 7. New Interface for Combining Elastography with RF Analysis. The user selects a region of interest (dotted box) in the pathology image and the software automatically selects the corresponding region from the RF data (left image) and elastogram (right image). The results of RF analysis, texture analysis, and the elastographic strain are all placed in the database for cancer or benign depending on the ROI type selected in the center pull down menu.

The user draws boxes around each image to inform the software of the relative sizes of the prostate in each image so that the software can find corresponding regions on each image. This method eliminates problems from distortion of the image in the vertical direction that can occur in elastography. The software also allows the user to adjust the display of the elastogram since the elastographic data may not always give a pleasing image without grayscale processing.

The new software represented a significant programming change in that the tools used (Matlab Guide) are different from the previous version of software. This necessitated a significant rewrite of code but yields benefits when further modifications to the user interface are required. For example, the interface above has been further modified in 2002 to incorporate features that improve the usability and appearance of the software (figure 8).

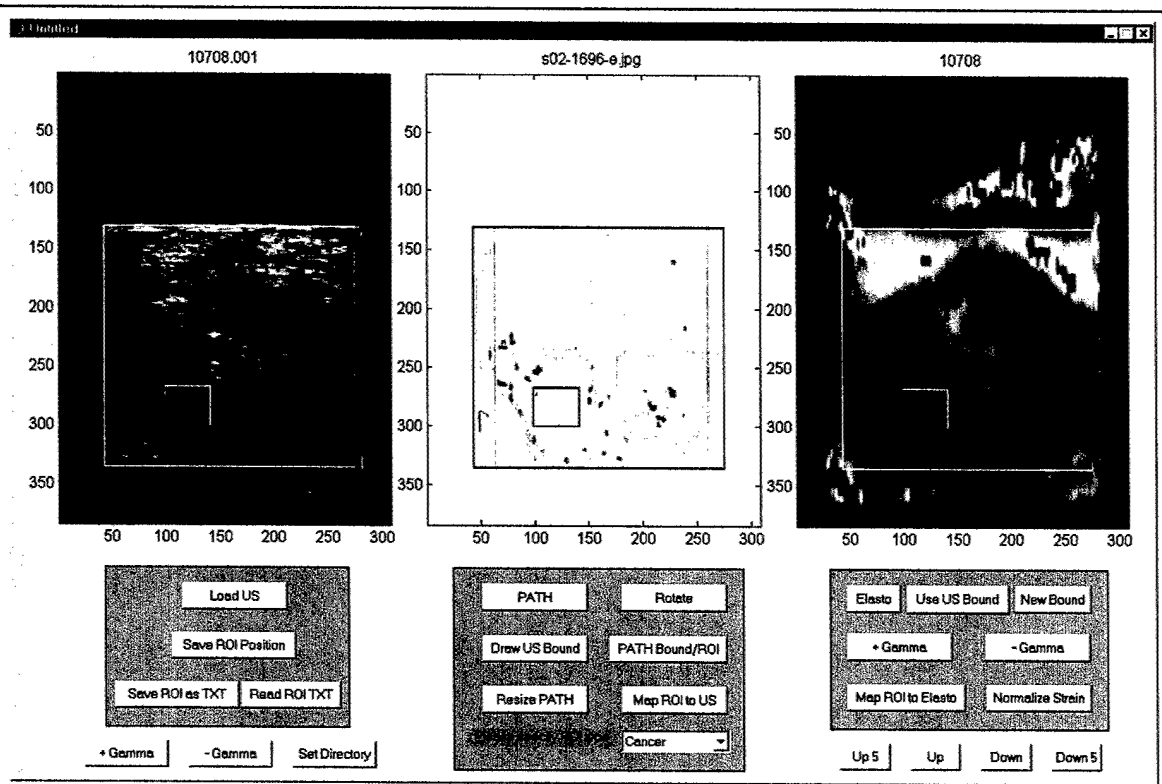

Figure 8: Newest GUI Interface for Prostate Data Registration. Note that distortion of the pathology image and of the elastogram are reduced or eliminated compared with Figure 7. Also, extra buttons for commonly manipulations have been added. A region of interest has been drawn in the cancerous region of the prostate gland and corresponding regions were automatically drawn on the sonogram and elastogram.

The elastographic strain data were initially obtained from the elastographic image. This was not optimal since the image represents a window into the large range of actual strain values mapped onto only 256 levels. By April 2002, the unwindowed strain values generated by the elastogram software were used. We have decided not to try to compute elastograms during ROI generation since the process is computationally intensive and time consuming. It will continue to be performed before the ROI selection software is run.

One issue of great concern is the quality of the elastographic data. Since the prostate glands are not embedded in gel as were the glands scanned by other investigators in animal work, there is great potential for lateral decorrelation which increases the noise in elastograms and decreases the contrast between benign and malignant tissue. Software with improved ability to correct for lateral motion was expected from the University of Texas by April 2001. A version finally arrived in October 2001 but did not properly perform lateral correction. Elastography software problems and personnel problems at Texas prompted us to look into developing our own elastography software in conjunction with Dr. Konofagu at Harvard University. Dr. Konofagu did not have the time to commit to the project however and in October 2002, we reached a software sharing agreement with Remi Souchon in Lyon, France to use his elastography software in return for our pathology registration software and advice on how to properly present clinical prostate elastograms. We have completed preliminary tests of the new software and have recently supplied Mr. Souchon with additional RF data to further test his software on our data.

This software, like ours, runs in MATLAB so we should have little difficulty integrating the matrix output of that software with our data fusion/registration software. Also, since the Lyon group, headed by Jean Yves Chapelon (Inserm Therapeutic Ultrasound Research Laboratory, 69424 Lyon Cedex 03, France, u556@lyon151.inserm.fr) is the only other group known to us that is doing extensive prostate elastography and is also doing clinical prostate elastography, we feel that sharing information will produce high quality clinical elastograms sooner for both groups.

Another issue with elastography that was mentioned previously is the problem of quantifying what have been regarded as qualitative images. Our plan was to use the change in thickness of the overlying standoff pad as a means of normalizing the strain values and we spent most of the first half of 2002 trying to get this method to work. We modified the data acquisition routine to enable us to compute the pad thickness change, using various methods and winding up with a complex two pad approach (figure 9). As the transducer compressed the prostate gland, the change in standoff pad thickness was measured by monitoring a change in separation of the signal peaks corresponding to the pad-pad interface and the pad-prostate interface (figure 10).

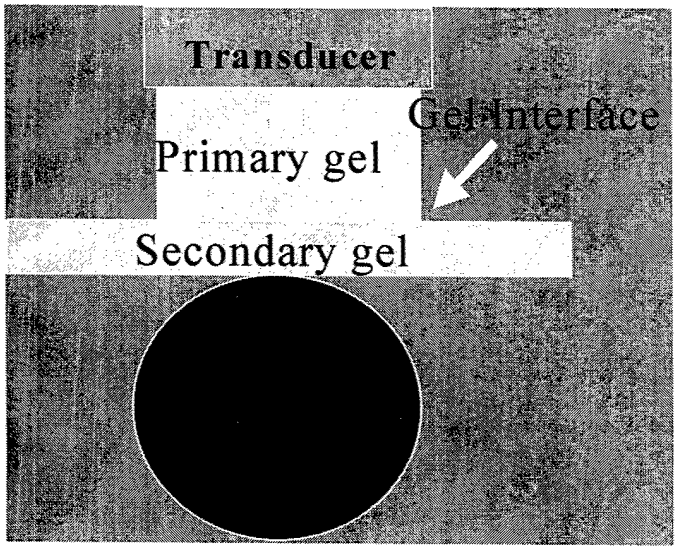

Figure 9: Setup of gel pads for estimation of gel pad thinning during elastography

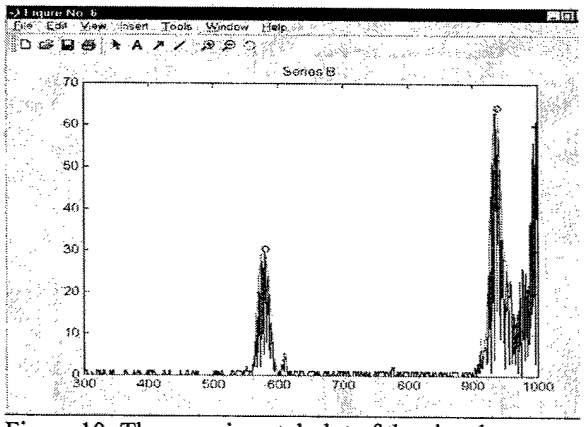

Figure 10: The experimental plot of the signal amplitude. The small peak represents the interface between the primary and secondary gel pads whereas the much larger peaks to the left represent the secondary gel pad-tissue interface. Horizontal axis is # of data points away from transducer. Y axis = amplitude.

It was felt that the secondary gel pad, being unconstrained by the plastic block containing the primary gel pad would be softer and would thin to a greater extent during compression than would the primary gel pad. Unfortunately, the somewhat greater stiffness of the gel pads compared to the prostate gland resulted in pad thinning that was too small for us to reliably measure either by peak detection methods or by cross-correlation methods. Table 2 shows the results of several methods we tried. The best method was a leading edge detection algorithm but this method at best still gave at least an 11% standard deviation in measurement reproducibility studies using a prostate phantom made of beefsteak. The local maximum detection algorithm was at times wildly inaccurate producing a 1270% standard deviation in the measurement

reproducibility studies. With such large variability, using gel pad thickness as a normalization factor to reduce variability in average strain in elastograms might actually increase variability rather than decrease it. We looked again at the factors causing variability in average strain. These factors can be organized into three different sources: those produced by differences in tissue, those produced during acquisition, and those introduced by the method used to estimate strain.

BEEF PHANTOM GEL COMPRESSION ESTIMATION

MEAN (% SD) for .4 or .5mm comp.

	ESTIMATOR		
DISTANCE	LEADING EDGE	LOCAL MAXIMUM	PARABOLIC FIT
Transducer to Tissue	-1.4 (71)	-2.6 (231)	------
Transducer to Gel interface	-9.58 (11)	-8.15 (27)	-8.64 (16)
Gel interface to tissue	-7.4 (97)	-1.2 (1270)	-30.5 (88)

Table 2: Performance of gel pad thinning estimators for the two-gel pad system shown in Figure 9.

The tissue factors were the ones we were trying to see, so it would make no sense to suppress those. The strain estimator might introduce errors, but there was no way to quickly change strain estimators. In the data acquisition category, four sources of potential variability were identified: 1) variable motor acceleration, 2) stiffness of the tissue holder, 3) gel pad standoff stiffness and fit, 4) variable precompression. The first three were being reasonably well controlled, but we were only crudely controlling precompression by watching the transducer indent the prostate gland while manually setting precompression. Another set of phantom tests was next conducted using manual control of precompression and also computer controlled precompression. The results (table 3) show that computer control of precompression achieved the desired result of low mean strain variance (3.4%) whereas visual-manual precompression control yielded large standard deviations of 176% to 244%. Standoff pad thickness varied widely even when average strain variance in the prostate was low confirming the lack of reliability of gel pad thickness measurements.

Xducer – Gel Interface dist	-0.15 (185)	------
Xducer – phant distance	0.31 (176)	-0.49 (167)
Avg Phant Strain	.022 (244)	.0068 (3.4)

Table 3: Comparison of manual vs. computer controlled precompression.. Gel pad thicknesses were measured as well as the average strain in the beefsteak prostate phantom.

The discovery that computer controlled precompression could markedly reduce strain measurement variability forced us to acquire a new set of prostate glands using this method of acquisition. We are now at the end of the repeat acquisitions and are ready to begin acquisitions anew as outlined in task 6.

Task 6 (months 7-18): More prostate data collection.

As mentioned in the previous section, software from the University of Texas expected to allow acquisition at higher compressions for higher image quality did not meet expectations and because of personnel problems at UT, hopes for new software have faded. Our new collaboration with the Lyon group promises to give us the capability to do lateral corrected elastograms, which should improve image quality and allow the efficient use of a curved array transducer, where lateral motion correction is nearly mandatory because of the lateral forces generated by the curved transducer face. We have not wanted to begin acquisition with the curved array until the elastography problems were solved since we would run the risk of being unable to monitor the quality of our acquisitions and might get into a situation similar to that we experienced with RF data acquisition—having to repeat acquisitions because of deficiencies in data acquisition or because a modification in acquisition methodology is required to optimize the elastogram.

In the past month, we have begun testing the setup that would be used for curved array acquisition in the past month. The best configuration seems to be one where the long transrectal probe is mounted vertically in the motorized transducer holder and the standoff pad (still required to avoid noise in the near field of the transducer) is simply laid across the top of the prostate gland in the water bath (figure 11). Some modification to the registration software to accommodate a sector (pie shaped) scan will be required but this polar to rectangular coordinate conversion is a preprogrammed function in MATLAB.

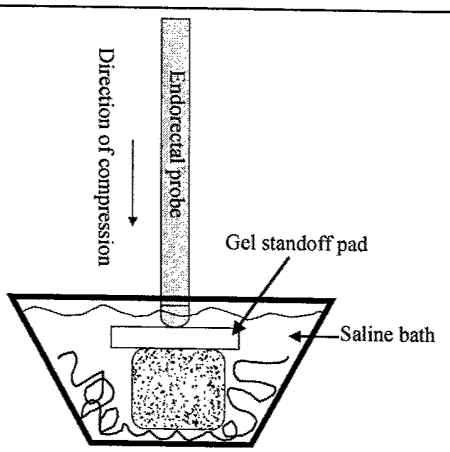

Figure 11: Current setup for curved array transducer prostate RF acquisition.

In summary, we still have not begun acquisition of curved array RF data but this is primarily because of our focus on resolving elastography issues and the need to acquire new linear array data as a result of a change in acquisition procedure. With the lateral correction elastography issues on the way to resolution, we have begun limited curved array acquisitions on prostate glands and will begin performing the dual linear array, curved array acquisitions after three or four more test runs. We still plan on acquiring and processing curved array data for at least the next six to nine months.

Task 7 (months 11-22): Compute RF and texture features for all stage 1 acquisitions.

RESULTS

During 2001, computation of RF and Texture Features on approximately 75% of the data existing at the time was completed. Potentially useful features were identified using the Mahalanobis distance as an index of the usefulness of both single features and feature combinations for separating benign from cancerous tissue. Figure 12 shows the experimental setup used:

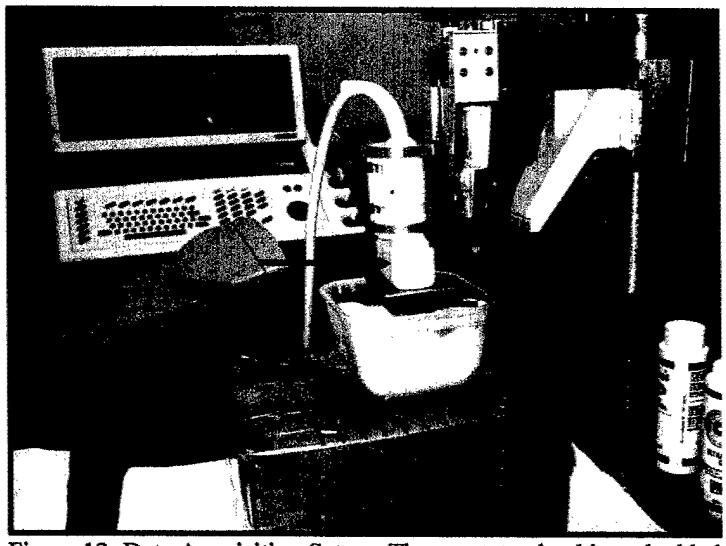

Figure 12: Data Acquisition Setup. The prostate gland is embedded in toweling and flooded with normal saline. The ultrasound probe (long black arrow) is held vertically and compresses the gland driven by a computer controlled stepper motor. The standoff gel block is held in place by the reddish orange plastic block (short black arrow) attached to an aluminum pressure plate attached to the transducer.

At total of eight different RF and texture features were computed from selected regions of interest. Features based on the RF data included the slope of backscatter vs. frequency, the zero frequency intercept of the backscatter intensity, and the mid bandwidth value for backscatter[3]. One feature based on image statistics was computed, this was the image signal to noise ratio (μ/σ)[4]. Four image texture features based on the co-occurrence matrix were computed: angular second moment, entropy, contrast, and correlation[5]. The features were computed from 36 cancer regions of interest and 19 benign regions of interest. Table 4 shows the mean and standard deviations for the various features.

Table 4. Feature Values for Benign and Malignant Prostatic Tissue—variable sized ROIs

FEATURE	CANCER (Mean ± s.d.)	BENIGN (Mean± s.d.)
Slope	0.778 ± .348 dB/MHz	.588 ± .326
Intercept	-11.81 ± 2.19 dB	-10.41 ± 2.20
Mid Band Value	-7.88 ± 1.48 dB	-7.42 ± 1.57
Signal to Noise Ratio	1.62 ± .38	1.36 ± .35
Angular Second Moment	.0099 ± .018	.0029 ± .0026
Entropy	-5.4 ± 1.04	-6.42 ± .78
Contrast	4111 ± .38	2066 ± 1049
Correlation	-.7469 ± .115	-.8043 ± .0788

The Mahalanobis distance is a measure of the statistical distance between two clusters of values relative to the scatter or variance of those values. To provide good discriminability between

benign and cancerous prostate tissue, the Mahalanobis distance should be maximized. Table 5 shows the Mahalanobis distance between cancer and benign tissue using linear discriminant analysis and various features or feature combinations. The discriminant analysis was performed using Minitab R13 software using the leave-one-out (cross-validation) method. This method minimizes the optimistic bias that results from using the same data for both training and performance estimation.

Table 5. Feature Performance for Cancer vs. Benign

FEATURE (S)	MAHALANOBIS DISTANCE
Slope & Intercept	0.418
Intercept & Entropy	1.351
Slope & Entropy	1.498
Intercept & Contrast	0.765
Entropy & Contrast	1.14
Slope	0.309
Intercept	0.403
Signal to Noise, Slope, Entropy	1.700

As is usually the case, more features lead to larger values and greater separation. But with the limited data set at hand, it is appropriate to use no more than 2-3 features to avoid an optimistically biased estimate of performance for the task of separating cancer from benign tissue. Receiver operating characteristic analysis was applied to the best two-feature combination, slope and entropy. The resulting area under the ROC curve was Az = .77, far from ideal but still encouraging.

REGION OF INTEREST DEPENDENCE

During the analysis, it was noted that the size of the region of interest used could affect the results—especially for SNR and the texture features. Since benign regions of interest tended to be larger than cancer regions, some of the difference in features could be the result of ROI size. To eliminate this effect, we have modified the software so that regardless of the size of ROI chosen by the human observer, the features are all computed from sub regions of identical size (approx RF lines wide). For a large region of interest, more subregions are present but this no longer affects the mean value, only the variance and Standard Error of the Mean.

The dependence of texture features and statistical image features on the size of the region of interest chosen has been known for some time although it is often ignored when experiments showing the value of those features are reported. It is not generally known that RF features such as backscatter and signal to noise ratio can be biased by use of variable sized regions of interest. This important topic has not been systematically studied but the need is real. For this reason and because of his first hand experience with this effect, Mr. He has chosen to continue his studies to obtain a Ph.D. and his thesis topic will be to explore this effect using our prostatic data plus additional phantom and simulation data.

Because of the focus on improving the quality of elastography and the need to acquire new prostate cases with altered acquisition procedures, we have only reprocessed the RF data using small fixed sized ROIs on a limited subset of cases and ROIs. Table 6 gives the feature values for 150 ROIs all approximately 1.9 x 2.3 mm in size. From the t-test results in the far right column, three features, entropy, angular second moment, backscatter slope, and cepstral energy

appear to be promising. When the full sized ROI's were processed for comparison, several features (mean, entropy, angular second moment and midband fit) gave much lower p values--- a good indication that ROI size was biasing the results since benign ROI sizes were significantly larger than cancer ROIs. Feature values for an additional three hundred small ROIs are being computed as part of a more comprehensive program to explore how feature values and variability change as ROI size is altered. The size of the fixed ROI used is an important issue. If we make them too small, then the computed values for some features could become very unstable but if they are too large, then our ability to detect small foci of cancer will be compromised. Only a systematic study of the problem will clarify what size or sizes of ROI are optimal

FEATURE	Benign Mean	Benign SD	Cancer Mean	Cancer SD	t test p- value
muoversigma	1.75	0.28	1.77	0.31	0.77
CoC Entropy	-3.86	0.19	-3.79	0.31	0.15
CoC Ang 2nd Moment	0.02	0.01	0.03	0.01	0.11
CoC Contrast	5843.41	2063.89	5749.17	2135.66	0.79
CoC Correlation	-0.70	0.08	-0.69	0.09	0.54
backscatter slope	0.04	1.53	-0.29	1.72	0.23
backscatt intercept	-36.11	9.81	-35.37	8.52	0.62
midband fit	-35.90	7.14	-36.80	9.82	0.54
Wtd Avg Cepstral Peaks	2.39	0.38	2.41	0.41	0.69
Wtd Avg Magnitude of Peaks	1.90	0.12	1.88	0.13	0.56
Energy of low portion of Cepstrum	0.08	0.01	0.08	0.01	0.16
phase profile maximum	8.61	2.98	8.56	3.11	0.92
phase profile variance	1.61	0.30	1.61	0.30	0.99

Table 6: FEATURE VALUES FOR BENIGN AND MALIGNANT PROSTATE TISSUE --- FIXED ROI SIZE (90 BENIGN, 60 CANCEROUS)

EXTENT OF CANCER INVOLVEMENT

Another important issue has surfaced in our examination of the pathology. Cancer involvement of the prostate gland may be massive with solid sheets of tumor cells replacing normal tissue, or it may be only one or two cells embedded in normal prostate tissue, or it may be anything in between. Since our characterization features are likely to be dependent on the EXTENT of involvement of involved regions of the prostate gland, we may need to map out different levels of prostate cancer involvement on the microscopic images rather than just marking out areas of any cancer involvement. That way, if an intermediate feature value is obtained from a region of interest, it can be determined if the reason is that there is intermediate involvement with cancer rather than complete replacement of normal tissue by cancer. A thorough exploration of this complex issue is beyond the scope of this project, but we plan to begin some preliminary

investigations of it to help us determine how the subject should be studied. We believe that our carefully registered pathology and US data gives us a unique opportunity to study this problem...and the bigger problem of how texture, RF features and elastographic strain vary with varying degrees of replacement of normal prostate tissue by cancer.

SOFTWARE QUALITY ASSURANCE

A big concern throughout the project has been software checking for correct computation of the texture and RF features. Several months during 2002 were spent checking the computation of RF features using two methods: 1. Scans of phantoms of known properties to check the backscatter computations, 2. Crosschecks with another investigator using the same RF data to see if results match. Method #1 revealed some significant coding errors in our calculations of backscatter vs. frequency that have been corrected. These results were checked by Keith Wear of the FDA who is satisfied that the computations are now correct. Method #2 was (and is) performed in conjunction with Ms. Jun Yang, an investigator working on characterization of breast masses at George Washington University using similar features to ours. Mr. He and Ms. Yang are now periodically checking their computations using identical RF data sets to help eliminate coding errors. When an anomaly surfaces that neither can explain, the issue is referred to Dr. Guo (Jun Yang's supervisor), Dr. Wagner, or Dr. Wear or the PI for resolution.

CLASSIFIER DEVELOPMENT

Up to now, we have taken a conservative approach to actual classifier development using primarily a linear Bayesian classifier. Dr. Wagner, our team member specialist on classifiers, prefers a conservative classifier to one that is complex and whose properties are less well understood. Other investigators have found that a linear Bayes classifier does not provide adequate differentiation of benign from malignant tissues in the prostate and use a neural network classifier. Dr. Lo on our team is ready to proceed with a neural network classifier as soon as we provide him with a volume of high quality data. Jun Yang has used a k-nearest neighbor classifier with success in her breast work, and Mr. He will work with her to develop that classifier for our data set. This process will begin as soon as all the ROIs are selected (about 80% complete for the linear array data) and the features are computed.

In summary, we have completed processing of a considerable portion of the RF data and the results are promising. Using the knowledge we acquired performing that processing, we are acquired some additional data and have modified the way we compute the features to remove bias and increase reliability. In the past year we focused on improving the reliability of the elastographic strain feature and will be exploring issues such as extent of tumor involvement and ROI size in future work.

Task 8 and Task 9 (months 13-26 and 24-30): Acquire RF with a curved array transducer.

As mentioned in Task 6, collection of data using a curved array transducer just begun. The software developed for linear array data will require some modification so that the correct region is obtained from the ultrasound data once the pathology image region of interest is selected. This

problem (one of scan conversion—i.e. polar to rectangular coordinate conversion) should be solvable in a short period of time. The curved surface of the transrectal probe will produce a stress that decays more rapidly as a function of depth. Since using gel standoff compression to normalize strain data has been abandoned, the plan to measure standoff distances along each A-line has also been eliminated. Once we have more data, we will be able to determine if a correction for more rapid stress field decay is necessary.

While we anticipate having the resources to continue our research beyond this point and to acquire an additional 50 prostates using linear array and curved array transducers, our ability to acquire an additional 50 beyond that point using non parallel scan planes is much more uncertain. That phase which generates a 3D US data set from non parallel scans is less critical since new 3D ultrasound technology has been commercially developed since 1998 that essentially duplicates that work. The parallel plane data should be adequate for demonstrating the feasibility of using combined features to detect cancer.

RESEARCH ACCOMPLISHMENTS

- Software has been developed under this program that can reliably find ultrasound data corresponding to an area of pathology on a pathology image. This technique could have broad applicability to any situation where in-vitro scans are being correlated with pathology.
- Software for computing both RF based and image texture based features for prostatic tissue or any other tissue has been developed and tested.
- Preliminary analysis shows that the features are promising and suggest that RF and texture based features can be used to discriminate between cancer and benign tissue. Discriminability will hopefully be further enhanced by adding elastography.
- Preliminary results show that bias in ROI size can bias both RF and texture feature values so that the features appear to be able to separate benign from cancerous tissue when such is not really the case. This topic will be Mr He's Ph.D. thesis and a manuscript is being prepared on the subject.
- Software to combine elastographic strain data with RF and texture features has been developed and refined.
- The problem of how to reduce variance in elastographic strain data has been examined and a solution found for in-vitro work. The knowledge that variable precompression is the main factor that must be controlled to obtain reproducible strain estimates in tissue is key for future work on in-vivo elastography.
- A strong collaboration with the only other group worldwide doing large numbers of prostate elastograms has been formed and promises to advance the field of prostate elastography significantly more rapidly than would otherwise be the case.
- The equipment used for this project is also being used for work on in vivo elastography in the study of the effects of acupuncture on connective tissue at the site of needle insertion (collaboration with Dr. Helene Langevin, Division of Neurology, Department of Medicine, UVM College of Medicine).

REPORTABLE OUTCOMES

1. Database of completely sectioned prostate glands with all cancer foci located plus correlated ultrasound raw data. This is a valuable resource that may be used for studies of the distribution of cancer and for any study requiring ultrasound image or raw data that can be precisely correlated with histology. The combining of this data set with the AFIP data set will produce a larger and more reliable data set than now exists for estimation of the probability of cancer as a function of location in the gland.
2. Abstract: He Z, Skljarevski G, Trainer T, Tuthill JM, Wagner RF, Huston D, Garra BS. Classification of benign and malignant prostate tissue using radio frequency ultrasound data: preliminary results of in vitro studies of radical prostatectomy specimens. Ultrasonic Imaging 2000;22:238. ----- see Appendix 1.
3. Abstract: He Z, Grimm SE, Padmanibahn V, Trainer TD, Tuthill JM, Wagner RF, Wear KA, Huston D, Garra BS. In vitro identification of prostate cancer in radical prostatectomy specimens: combining elastography and ultrasonic backscatter features. Ultrasonic Imaging 2000;22:171-197.
4. Presentation: He Z, Skljarevski G, Trainer T, Tuthill JM, Wagner RF, Huston D, Garra BS. Classification of benign and malignant prostate tissue using radio frequency ultrasound data: preliminary results of in vitro studies of radical prostatectomy specimens. Presented at the 26th International Symposium on Ultrasonic Imaging and Tissue Characterization, Rosslyn, VA, May 31 2001-----See Appendix 2
5. Presentation: He Z, Grimm SE, Padmanibahn V, Trainer TD, Tuthill JM, Wagner RF, Wear KA, Huston D, Garra BS. In vitro identification of prostate cancer in radical prostatectomy specimens: combining elastography and ultrasonic backscatter features. 27th International Symposium on Ultrasonic Imaging and Tissue Characterization. 3-5 June 2002, Arlington, VA.
6. Publication: Langevin HM, Churchill DL, Fox JR, Badger GJ, Garra BS, Krag MH. Biomechanical response to acupuncture needling in humans. J Appl Physiol 2001;91(6): 2471-8.
7. Publication: Langevin HM, Churchill DL, Wu J, Badger GJ, Yandow JA, Fox JR, Krag MH. Evidence of connective tissue involvement in acupuncture. FASEB J 2002;16(8):872-4.
8. Thesis: He, Zhi, Quantitative Sonographic Prostate Cancer Characterization, Masters of Science Thesis, October 2001 ----- See Appendix 3
9. Masters Degree Awarded October 2001 to Zhi He
10. Employment & Training Supported by this Project Funding:
    a. Masters Degree Training by Zhi He
    b. Doctoral Degree Training by Zhi He
    c. Part time Programmer: Steven Felker
    d. Half time Research Assistant: Sarah Grimm

CONCLUSIONS

Despite numerous delays and personnel difficulties, steady progress towards the ultimate goal of combining multiple US features together to aid in the detection of prostatic cancer has been made.

Our preliminary analysis of the RF data suggest that cancerous tissue can be differentiated from benign tissue using RF and texture features. Much of the RF data collected early in the project was of poor quality—caused by data acquisition beginning before replacements had been found for those originally responsible for developing the software to process and monitor data acquisition. This poor quality data has been replaced with new data of high quality and the focus in the last year of the project was to verify the quality of the data and of the software so that the combined features will have the best chance of accurately distinguishing cancer from benign tissue. With the development of a method to reduce measurement variation in elastography and the formation of an alliance with a group in France share software, we now are well positioned to add elastography and to proceed with analysis of curved array data.

In addition to supporting the Masters degree and PhD programs for Mr. Zhi He, we have accumulated a large database of matched ultrasound RF and pathology data that can be used for multiple future studies including the study of the distribution of cancer in the prostate, a study of the extent of replacement of normal tissue by cancer, and correlative studies of the effects of varying involvement by prostate cancer on ultrasonic backscatter, texture, and tissue elastic properties.

We have just begun acquiring data using a curved array transducer and are confident that the needed modifications can be made to our software so that it will work properly with the new transducer array. We remain confident that we will be able to produce probability images showing areas likely to contain cancer using the combination of RF, texture, and elastographic features. We have the resources to continue this work beyond the official end of the contract and will be pleased to file an addendum to this report in six to nine months with additional results.

REFERENCES

[1] He Z, Skljarevski G,Trainer T, Tuthill JM, Wagner RF, Huston D, Garra BS. Classification of benign and malignant prostate tissue using radio frequency ultrasound data: preliminary results of in vitro studies of radical prostatectomy specimens. 26th International Symposium on Ultrasonic Imaging and Tissue Characterization, 30 May –1 June 2001, Arlington, VA.
[2] He Z, Grimm SE, Padmanibahn V, Trainer T, Tuthill JM, Wagner RF, Wear KA, Huston D, Garra BS. In vitro identification of prostate cancer in radical prostatectomy speciments: combining elastography and ultrasonic backscatter features, 27th International Symposium on Ultrasonic Imaging and Tissue Characterization, 3-5 June 2002, Arlington, VA.
[3] Feleppa EJ, Liu T, Kalisz A, Shao MC, Fleshner N, Reuter V, Fair WM. Ultrasonic spectral parameter imaging of the prostate. Int J Imaging Syst Technol. 1997;8:11-25.
[4] Wagner RF, Smith SW, Sandrik JM, Lopez H. Statistics of Speckle in ultrasound B-scans. IEEE Trans. Sonics Ultrason. 1983;SU-30:156-163.

[5] Garra BS, Krasner BH, Horii SC, Ascher S, Mun SK, Zeman RK. Improving the distinction between benign and malignant breast lesions: the value of sonographic texture analysis. Ultrasonic Imaging 1993;15:267-285.

APPENDICES

APPENDIX 1: LIST OF PEOPLE PAID UNDER THE CONTRACT

APPENDIX 2: SLIDE PRESENTATION 2002

Appendix 1
Persons Paid Under Contract DAMD17-99-1-9007

1. Brian S. Garra, PI
2. Richard (Zhi) He
3. Gorana Skjlarevski
4. Sarah Grimm
5. Jonathan Ophir
6. Steven Felker

APPENDIX 2:

Slide presentation 6-2002 at the International Tissue Characterization Symposium, Arlington, VA

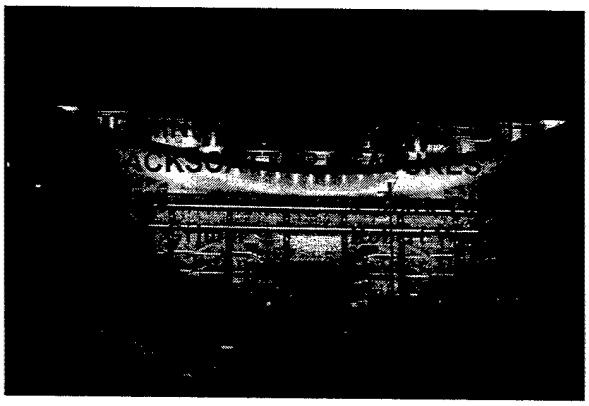

This Work Supported By:

Department of Defense Contract
DAMD –17-99-1-9007

PREVIOUS WORK

- Registration of Pathology and RF Ultrasound Data
- Computation of RF Backscatter Features from Benign and Cancerous Prostate Regions

REGION OF INTEREST GENERATION

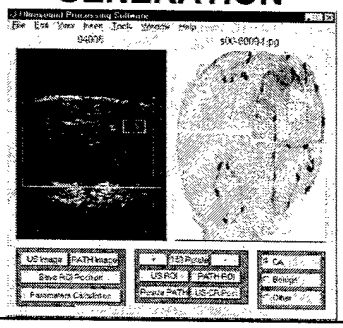

PREVIOUS RESULTS
RF & IMAGE ANALYSIS

Feature	CA Mean (±s.d.)	Benign Mean (±s.d.)
Slope	0.778±.348 dB/MHz	.588±.326
Intercept	-11.81±2.19 dB	-10.41±2.20
Mid Band	-7.88±1.48 dB	-7.42±1.57
SNR	1.62±.38	1.36±.35
ASM	.0099±.018	.0029±.0026
ENT	-5.4±1.04	-6.42±.78
CON	4111±3872	2066±1049
COR	-.7469±.115	-.8043±.0788

CURRENT GOAL:
ADD ELASTOGRAPHIC STRAIN TO THE RF & IMAGE FEATURES

PROBLEMS:

1. Elastograms are non quantitative—depict only relative stiffness
2. "Brightness" (strain) on elastograms varies from slice to slice
3. No fat available as reference tissue
4. Must reduce strain variance to use it in Bayesian or neural net classifier

SLICE TO SLICE STRAIN VARIABILITY

CASES	# SLICES	AVG STRAIN	%SD
102-107	67	.0035	65.7
113-115	52	.0155	182

INTEGRATING ELASTOGRAPHY

STEP 1: Register Strain Matrix With RF and Pathology

1. Precompute strain matrices
2. Adjust size of US and Elastogram to match pathology image
3. Select region of interest (ROI) in pathology image
4. ROI's drawn on US and Elastogram--- corresponding RF and strain data selected for processing

ROI SELECTION USING NEW GUI

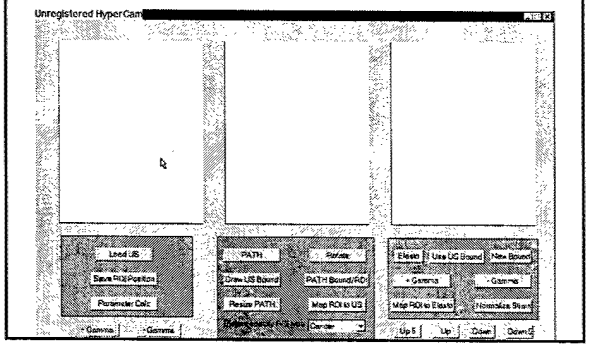

INTEGRATING ELASTOGRAPHY

STEP 2: Reduce the Variance of Numerical Strain Values

STRAIN VALUES

SOURCES OF VARIABILITY

- Tissue
  - Different tissues (i.e. cancer vs. hyperplasia vs. nl)
  - Non linear & variable response to compression
- Data Acquisition
  - Variable compression: Motor acceleration
    Tissue holder stiffness
    Gel standoff stiffness and fit
  - Variable precompression
- Strain Estimation
  - RF Decorrelation: Large axial displacement
    Lateral or elevational movement
    Misidentification of displacement

HYPOTHESES

- Commercial Gel Standoff Pads Have a Consistent Stiffness
- Measured Compression of the Gel Pad Will Give Some Indication of the Amount of Compression Used

EXPERIMENTAL METHOD

- InVitro Prostate Gland Tests – Two compressions at .3mm per compression
- Phantoms (Beef and Tofu)
  - Two compressions at both .3mm/compression and .5mm per compression
  - 4-20 acquisitions at each location on phantom
- One or Two Layer Gel Pad Standoff

EXPERIMENTAL METHOD II
ESTIMATION OF GEL PAD COMPRESSION

- Three Different Measurements Were Tried
  - Xducer to tissue
  - Xducer to gel interface
  - Interface to tissue
- Three Different Estimators of Pa[redacted] Were Tried
  - Leading edge of specular echo
  - Local Maximum of specular echo
  - Maximum of parabolic fit to peak of specular echo

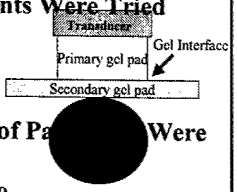

PAD THICKNESS ESTIMATION
EXPERIMENTAL EXAMPLE

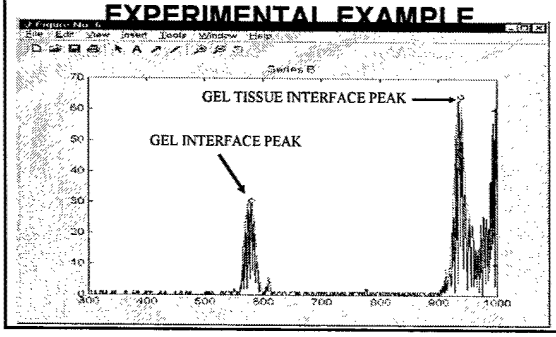

BEEF PHANTOM GEL COMPRESSION ESTIMATION
MEAN (% SD) for .4 or .5mm comp.

	ESTIMATOR		
DISTANCE	LEADING EDGE	LOCAL MAXIMUM	PARABOLIC FIT
Transducer to Tissue	-1.4 (71)	-2.6 (231)	------
Transducer to Gel interface	-9.58 (11)	-8.15 (27)	-8.64 (16)
Gel interface to tissue	-7.4 (97)	-1.2 (1270)	-30.5 (88)

A NEW HYPOTHESIS

- Variation in Pad Compression is at Least Partly Due to Changes in Tissue or Phantom Hardness
- Tissue/Phantom Hardness Changes Could be Due to Variations in Precompression

A NEW EXPERIMENT TO STUDY PRECOMPRESSION

- One or Two Gel Pads
- With & Without Controlled Pre compression

	Mean Value (% SD)	
Xducer – Gel Interface dist	-0.15 (185)	------
Xducer – phant distance	0.31 (176)	-0.49 (167)
Avg Phant Strain	.022 (244)	.0068 (3.4)

CONCLUSIONS

- Gel Pad Thickness Change Estimates are Too Variable to be Used as an Indicator of Compression
- Precompression is a Major Source of Variability in Strain Estimates
- Controlled Precompression is a Promising Way to Reduce Variation in Strain Estimates
- Further Study & Acquisition of Elastograms With Controlled Precompression is Needed & May be Useful For Correcting Older Prostate Strain Data